Psychophysiology, 51 (2014), 285–289. Wiley Periodicals, Inc. Printed in the USA.

DOI: 10.1111/psyp.12153

BRIEF REPORT

Synchronized network activity as the origin of a P300 component in a facial attractiveness judgment task

YUAN ZHANG,[a,b] AKAYSHA C. TANG,[b] AND XIAOLIN ZHOU[a,c,d]

[a]Center for Brain and Cognitive Sciences and Department of Psychology, Peking University, Beijing, China
[b]Department of Psychology and Department of Neuroscience, University of New Mexico, Albuquerque, New Mexico, USA
[c]Key Laboratory of Machine Perception (Ministry of Education), Peking University, Beijing, China
[d]PKU-IDG/McGovern Institute for Brain Research, Peking University, Beijing, China

Abstract

Many studies have used the P300 as an index for cognitive processing and neurological/psychiatric disorders. Here, we combined the source separation and source localization methods to investigate the cortical origins of the P300 elicited in a facial attractiveness judgment task. For each participant, we applied second-order blind identification (SOBI) to continuous EEG data to decompose the mixture of brain signals and noise. We then used the equivalent current dipole (ECD) models to estimate the centrality of the SOBI-recovered P300. We found that the ECD models, consisting of dipoles in the frontal and posterior association cortices, account for 96.5 ± 0.5% of variance in the scalp projection of the component. Given that the recovered dipole activities in different brain regions share the same time course with different weights, we conclude that the P300 originates from synchronized activity between anterior and posterior parts of the brain.

Descriptors: ERP, P300, SOBI, Facial attractiveness, Localization

The classical P300 is a positive-going event-related potential (ERP) component, which reaches its maximum at 300 ms (or more) after the presentation of a stimulus. It was first reported in a cue-target task in which participants were uncertain about the modality of the upcoming target (Sutton, Braren, Zubin, & John, 1965). The P300 component is observable in many tasks, such as target detection (Polich, 2007), outcome evaluation (Leng & Zhou, 2010; Wu & Zhou, 2009), and assessment of facial attractiveness (Schacht, Werheid, & Sommer, 2008; Werheid, Schacht, & Sommer, 2007). The P300 component is considered to be a neural signature of cognitive processes, and its variations can be used as markers for neurological and psychiatric disorders (Polich, 2007).

In the electroencephalogram (EEG) literature, the cortical origins of P300 are mainly investigated in studies employing the oddball paradigm or variations thereof (Linden, 2005), leaving a gap in the literature regarding the P300's generation beyond the oddball paradigm. Here, we elicited P300 responses in a task in which participants were first required to judge the attractiveness of a blurred face and then received an unblurred face as feedback for their judgment (Zhang, Li, Qian, & Zhou, 2012). There were two experimental factors: the first factor was attractiveness (attractive vs. unattractive), which referred to the facial attractiveness of feedback faces; the second was consistency (consistent vs. inconsistent), which referred to the attractiveness of feedback faces and whether or not they were consistent with participants' initial judgments of the blurred faces. In the previous study (Zhang et al., 2012), ERPs locked to the feedback faces showed that the P300 was more positive for faces consistent with than for faces inconsistent with the initial judgment, and was more positive for attractive faces than for unattractive ones. There was no interaction between attractiveness and consistency. These results suggested that the P300 can simultaneously encode different attributes of feedback. In the current study, we further investigated the functional significance of the P300 based on both its spatial origins and how it is modulated by experimental factors. We first applied a source separation algorithm to isolate the P300 component; we then used its scalp projection as input for source localization. In particular, we applied the second-order blind identification (SOBI; Belouchrani, Abed-Meraim, Cardoso, & Moulines, 1997) procedure to the continuous EEG data to isolate functionally distinct P300 sources for further investigation of their neuronal generators.

SOBI is a blind source separation algorithm that can be used to decompose scalp EEG signals into a set of putative recovered neuronal sources (i.e., SOBI-recovered components). Recent work has shown that SOBI is effective and robust in separating EEG data into physiologically interpretable components (Lio & Boulinguez,

This study was supported by the National Basic Research Program (973 Program: 2010CB833904) from the Ministry of Science and Technology of China and by grants from the Natural Science Foundation of China (30110972, 91232708). Miss Yuan Zhang was also supported by a Chinese Council Scholarship. We thank two anonymous reviewers for their constructive comments and suggestions concerning an earlier version of the manuscript.

Address correspondence to: Xiaolin Zhou, PhD, Department of Psychology, Peking University, Beijing, 100871, China. E-mail: xz104@pku.edu.cn

2013; Tang, 2010; Tang, Sutherland, & McKinney, 2005). Instead of simply minimizing the instantaneous correlation between recovered sources, SOBI quantifies their relatedness by simultaneously minimizing cross-correlations between all pairs of recovered sources and across all temporal delays (excluding autocorrelations; for details, see Belouchrani et al., 1997; Cardoso & Souloumiac, 1996). In this way, SOBI supports the use of temporal information contained in the EEG time series for source separation. Therefore, SOBI is capable of separating correlated neuronal sources, and a single SOBI component can be recovered when multiple brain regions share very similar time courses of activation through synchronization (Tang, 2010; Tang et al., 2005).

Method

The dataset used here was collected in our previous study (see Zhang et al., 2012, for more details). EEGs from 64 channels were recorded from 16 undergraduate students (eight female) during a facial attractiveness judgment task. EEG data were sampled at 512 Hz with a band-pass filter of 0.05–100 Hz. Before SOBI processing, time periods of rest and apparent noises were discarded from the dataset.

SOBI Processing

SOBI decomposes *n*-channel continuous EEG into *n* SOBI components, each of which corresponds to a recovered putative source that contributes to the scalp EEG signal. Each SOBI component has a time course of activation and an associated sensor space projection that specifies the effect of that putative source on each of the *n* electrodes.

Let x(t) represent the *n* continuous time series from the *n* EEG channels and x_i(t) the readings from the *i*th EEG channel. Because various underlying sources are summed via volume conduction to give rise to the scalp EEG, each of the x_i(t) can be assumed to be an instantaneous linear mixture of *n* unknown components or sources s_i(t), via the unknown $n \times n$ mixing matrix A. $x(t) = As(t)$. The putative sources, $\hat{s}(t)$, are given by $\hat{s}(t) = Wx(t)$, where $W = A^{-1}$. SOBI finds the unmixing matrix W through an iterative process that minimizes the sum squared cross-correlations between one recovered component at time t and another component at time $t + \tau$, across a set of time delays (Cardoso & Souloumiac, 1996; http://sig.enst.fr/~cardoso/). The following set of delays (τs, in ms) were chosen to cover a reasonably wide interval without extending beyond the support of the autocorrelation function: $\tau \in \{1, 2, 3, 4, 5, 6, 7, 8, 9, 10, 12, 14, 16, 18, 20, 25, 30, 35, 40, 45, 50, 55, 60, 65, 70, 75, 80, 85, 90, 95, 100, 120, 140, 160, 180, 200, 220, 240, 260, 280, 300\}$.

Identification of SOBI-Recovered P300 Candidates

We identified SOBI-recovered P300 candidates according to both their temporal and spatial characteristics. First, for each participant, using the averaged ERPs (band-pass filter of 0.1 – 30 Hz; epoch: –200 ~ 800 ms; baseline: –200 ~ 0 ms) evoked by unblurred faces, we selected a subset of P300 candidates based on temporal properties displaying a positive-going component with a peak amplitude of at least 2 μv and peak latency within 300 – 800 ms. Next, a second subset of P300 candidates was selected for each participant based on spatial properties displaying a symmetric scalp projection with a single broad dipolar field pattern. Typically, no more than five candidates result from using temporal criteria and no more than seven candidates result from using spatial criteria. Their overlap results in one P300 candidate in nine participants (56%) and two P300 candidates in seven participants (44%), which were further evaluated in source localization. For participants with two P300 components, we only report the one with maximal amplitude.

Source Analysis

The sensor space projections of P300 candidates, which are viewed as containing signals from a functionally distinct neuronal source, were used as inputs to BESA 5.0 (Brain Electrical Source Analysis; MEGIS Software, Munich, Germany) for source modeling. Because a SOBI component has fixed sensor weights, $\hat{a}^{(i)}$, the estimated dipole locations do not change with time. Equivalent current dipoles (ECDs) were fitted for P300 candidates within a standard ellipsoidal four-shell head model. ECD locations (mm) were found using a least squares algorithm and are reported in a Talairach coordinate system within the BESA standard brain.

Because of the largely symmetric scalp projection, bilaterally symmetric dipole pairs were used for ECD models. For each P300 candidate component, the number of dipole pairs and their initial positions were estimated based on the visual inspection on the current source density (CSD) map. CSD maps are the second spatial derivative of the voltage distribution and are considered better than the potential maps in visually revealing the underlying sources (Lagerlund, 1999). CSD maps typically exhibit sharp foci at scalp regions directly overlying nearby sources because of its insensitivity to currents arising from distant sources (Mitzdorf, 1985). As a result, the presence of a pair of strong, discrete CSD foci (a negative pole and a positive pole) indicate that a focal source lies between the poles. In the present study, symmetric dipole pairs were placed at estimated initial positions, and were allowed to move freely in the model-fitting procedure. To avoid the possibility that the solution was trapped in undesirable local minima, we repeated the model-fitting procedure four more times with different initial positions each time (i.e., placing all dipole pairs in the frontal, parietal, temporal, and occipital lobe, respectively). The finally chosen solution had to meet the following requirements: (a) goodness of fit was higher than 90%, and (b) the residual map showed no remaining prominent sources. If more than one solution resulted in goodness of fit higher than 90%, then the solution producing the least residual source was chosen.

Data Analysis

To investigate the functional significance of the P300 component, we conducted repeated measures analyses of variance (ANOVAs) with attractiveness and consistency as within-participants factors and P300 peak/latency as the dependent variable. For each participant, the electrode with the maximal weight was used for statistical analysis. Moreover, P300 peak and latency were calculated based on single trials for each participant; that is, peak and latency were first detected in the 300 ~ 800 ms time window for each trial, and then these values were averaged for each condition. The Greenhouse-Geisser correction was applied for the violation of the ANOVA assumption of sphericity.

Results

For each participant, we reliably found one SOBI-recovered P300 component, of which scalp projection, ERP waveforms, and CSD maps are presented in Figure 1. Temporally, the ERPs of these

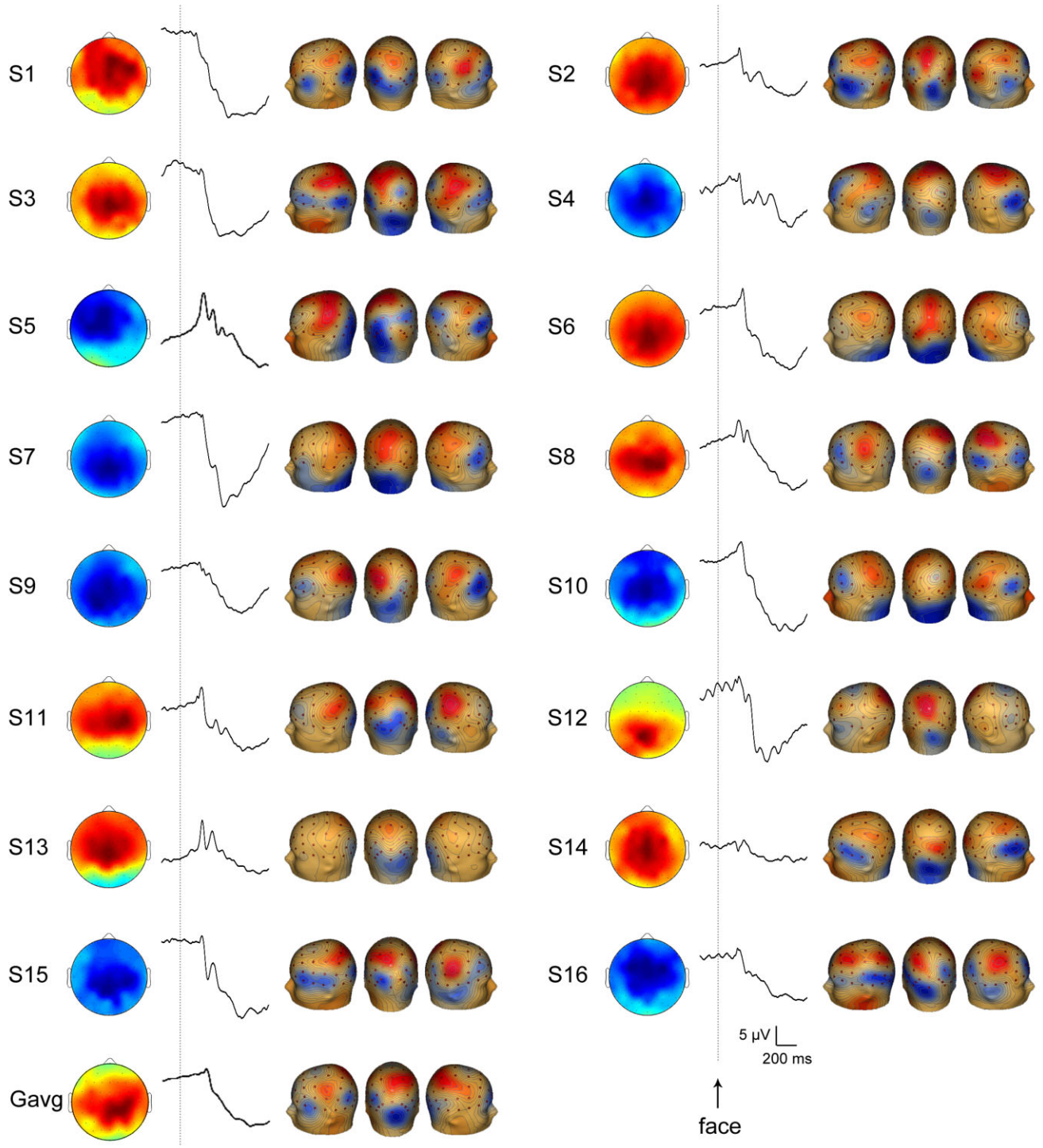

Figure 1. Scalp projection, ERP waveforms, and current source density (CSD) maps of the SOBI-recovered visual P300 component in each of the 16 participants (calbar: 5 μV, 200 ms). Scalp projections and ERP waveforms were the basis of identification for P300 candidates, whereas CSD maps were used in the estimation of dipole pair frequency and their locations. Vertical line indicates the onset of the unblurred face. Gavg = group average across all participants.

components displayed characteristic P300 responses, reflecting a positive-going waveform, which reached its maximum 14.4 ± 1.6 μv at 528 ± 31 ms postonset over participants. Spatially, the scalp projections were consistent with typical distributions of the P300 component, showing frontocentral ($n = 3$), central ($n = 8$), and centroparietal ($n = 5$) distributions.

The ECD models accounted for 96.5 ± 0.5% ($n = 16$) of the variance in the scalp projections of the SOBI-recovered P300 (Table 1), consisting of dipoles in the frontal (inferior frontal gyrus, $n = 12$; middle frontal gyrus, $n = 5$; superior frontal gyrus, $n = 1$) and posterior association cortices (angular gyrus, $n = 11$; precuneus, $n = 2$, supramarginal gyrus, $n = 1$; inferior temporal

Table 1. *Localizations of SOBI-Recovered Visual P300 Component for Each of the 16 Participants*

			Talairach coordinate (*x y z*)			
Subj #	GoF%	Pair of dipoles	Frontal lobe	Parietal lobe	Temporal lobe	Occipital lobe
1	93.7	3	58 38 23	52 −80 33		10 −82 −13 LG
2	98.6	4	42 24 16	43 −91 24		51 −87 −23
			47 58 27 MFG			
3	95.7	3	37 9 33	53 −73 32		35 −106 −3
4	95.1	4	53 31 27	47 −68 30		54 −81 −29
			23 −1 80 SFG			
5	97.8	3	63 25 38 MFG	27 −49 36		15 −107 8
6	98.4	3	24 5 16	48 −83 34		40 −96 −26
7	98.2	3	55 20 8	37 −85 43		27 −85 7
8	96.6	3	56 11 34	53 −39 44 SMG		10 −86 −8 LG
9	97.8	3	48 16 25	36 −81 28		35 −105 −7
10	96.1	3	51 31 6	31 −73 40		49 −86 −31
11	98.6	3	36 33 −13	30 −49 17 PCun		40 −96 27
12	97.4	3	46 48 43 MFG	11 −43 45 PCun		9 −114 −12 LG
13	99.2	3	30 19 12	33 −89 44		23 −76 5
14	95.7	3	53 25 35		75 −37 16 STG	27 −111 4
15	94.1	3	32 18 39 MFG		75 −39 9 STG	43 −79 31
16	91.2	3	46 60 6 MFG	42 −81 35	65 −43 −14 ITG	
Mean	96.5	3	45 22 19 IFG	41 −78 35 AnG	75 −38 13 STG	37 −93 −3 OCG
			47 42 31 MFG	21 −46 31 PCun		10 −94 −11 LG
SEM	0.5	0.1	3 3 4 IFG	3 4 2 AnG	0 1 4 STG	3 4 6 OCG
			5 9 7 MFG	10 3 14 PCun		0 10 2 LG
N			*n* = 12 IFG	*n* = 11 AnG	*n* = 1 ITG	*n* = 12 OCG
			n = 5 MFG	*n* = 1 SMG	*n* = 2 STG	*n* = 3 LG
			n = 1 SFG	*n* = 2 PCun		

Note. In the frontal lobe column, Talairach coordinates without an indicator refer to the inferior frontal gyrus; in the parietal lobe column, Talairach coordinates without an indicator refer to angular gyrus; in the occipital lobe column, Talairach coordinates without an indicator refer to the occipital gyrus. Subj # = participant ID; GoF = goodness of fit; IFG = inferior frontal gyrus; MFG = middle frontal gyrus; SFG = superior frontal gyrus; AnG = angular gyrus; SMG = supramarginal gyrus; PCun = precuneus; ITG = inferior temporal gyrus; STG = superior temporal gyrus; OCG = occipital gyrus; LG = lingual gyrus; *SEM* = standard error of mean; *N* = number of participants with P300 generators located in a specific brain region.

gyrus, $n = 1$; superior temporal gyrus, $n = 2$; occipital gyrus, $n = 12$; lingual gyrus, $n = 3$). For each individual, the recovered P300 dipole activities in the frontal and posterior regions shared the same time course with different weights, indicating that these brain regions cooperated via synchronization. In addition, we performed source localization using standardized shrinking LORETA-FOCUSS (SSLOFO), which is representative of the distributed source models. Localization results are similar to those based on ECD models.

Repeated measures ANOVAs revealed a significant main effect of attractiveness on the P300 latency, $F(1,15) = 9.16$, $p < .01$, with the P300 taking a longer time to reach its maximum for unattractive faces (565 ms) than for attractive faces (544 ms). The main effect of consistency was also significant, $F(1,15) = 19.92$, $p < .001$, with the P300 taking a longer time to reach its maximum for the inconsistent condition (566 ms) than for the consistent condition (544 ms). There was no interaction between attractiveness and consistency, $F(1,15) < 1$, $p > .1$. Our analysis of the P300 peak amplitude resulted in no significant effects. Note that the effects of attractiveness and consistency were observed on peak latency, rather than on peak amplitude as in Zhang et al. (2012). Methodological differences in source separation could have contributed to this difference. Principal component analysis (PCA) used in Zhang et al. (2012) was performed on ERPs averaged over trials in each condition, whereas SOBI was performed for each participant individually at a time based on continuous EEG data covering single trials. Compared with a PCA P300, which possibly has a mixture of neuronal sources and noise sources, an SOBI P300 has physiologically more interpretable neuronal sources. Moreover, given that SOBI can utilize temporal structures in the data (i.e., using a set of temporal delays), SOBI is capable of revealing variations in P300 latency across conditions that cannot be detected by PCA.

Discussion

The main purpose of this study was to investigate cortical generators of the visual P300 component measured in a facial attractiveness judgment task. Results revealed a relatively stable configuration of P300 generators across participants, including frontal, parietal/temporal, and occipital regions. Moreover, recovered activities of these generators shared the same time course with different weights, given the computational algorithms behind SOBI (Tang et al., 2005).

Cortical origins of the P300 component discovered in the current study overlapped considerably with those found in previous EEG studies. The frontal lobe, which is believed to be related to attention mechanisms, plays an important role in P300 generation (Polich, 2007; Swick, 1998). The temporal/parietal region is consistently reported to be involved in P300 generation (Polich, 2007; Schimpf & Liu, 2008), which is possibly associated with mechanisms for memory. The occipital lobe is also reported as a P300 generator in studies using visual stimuli (Lorenzo-López, Amenedo, Pascual-Marqui, & Cadaveira, 2008; Schimpf & Liu, 2008). Although each single brain region mentioned above is related to P300 generation, the P300 in the current study did not originate from any one single brain region; instead, it was generated from a distributed network consisting of frontal and posterior association regions. Importantly, the recovered dipole activities in

different brain regions shared the same time course of activation, suggesting that these brain regions cooperated via synchronization.

ERP results revealed that it took longer for the P300 to reach its maximum for unattractive faces than for attractive faces and for the inconsistent condition than for the consistent condition. The P300 latency is believed to be a sensitive measure of the time needed to evaluate visual stimuli (Polich, 2007). Compared with unattractive faces, attractive faces may have higher motivational significance and thus may capture attention more easily (Johnston & Oliver-Rodríguez, 1997; Schupp et al., 2000), facilitating attractiveness evaluation in working memory. Moreover, compared with the consistent condition, faces in the inconsistent condition may take a longer time to be encoded in working memory due to the process of conflict resolution. Therefore, it is possible that the frontal-posterior network, which generates the P300 component, supports the working memory operation during the evaluation of facial attractiveness and consistency. This suggestion is in line with a previous study showing that synchronization between frontal and posterior association cortices plays an important role in working memory processing (Sarnthein, Petsche, Pappelsberger, Shaw, & Von Stein, 1998); in working memory processing, relevant information is held and continuously updated in frontal areas, while sensory information is stored in posterior association cortices.

The scalp projections of the P300 component varied across participants. Both individual differences in processing the feedback faces and the unsteadiness of the physical positions of EEG channels on the head could contribute to this variation (Tang, 2010). Importantly, however, there existed a relatively stable configuration of P300 generators across these participants.

In conclusion, the present study found that (a) there exists a functionally distinct visual P300 component in facial attractiveness judgment after source separation; and (b) this P300 originates from synchronized activity between the frontal and posterior association cortices, which may be associated with working memory processes involved in the task.

References

Belouchrani, A., Abed-Meraim, K., Cardoso, J.-F., & Moulines, E. (1997). A blind source separation technique using second-order statistics. *IEEE Transactions on Signal Processing*, *45*, 434–444. doi: 10.1109/78.554307

Cardoso, J.-F., & Souloumiac, A. (1996). Jacobi angles for simultaneous diagonalization. *SIAM Journal on Matrix Analysis and Applications*, *17*, 161–164. doi: 10.1137/S0895479893259546

Johnston, V. S., & Oliver-Rodríguez, J. C. (1997). Facial beauty and the late positive component of event-related potentials. *Journal of Sex Research*, *34*, 188–198. doi: 10.1080/00224499709551884

Lagerlund, T. D. (1999). EEG source localization (model-dependent and model-independent methods). In E. Niedermeyer & F. Lopes da Silva (Eds.), *Eletroencephalography: Basic principles, clinical applications, and related fields* (pp. 809–822). Baltimore, MD: Lippincott, Williams and Wilkins.

Leng, Y., & Zhou, X. L. (2010). Modulation of the brain activity in outcome evaluation by interpersonal relationship: An ERP study. *Neuropsychologia*, *48*, 448–455. doi: 10.1016/j.neuropsychologia.2009.10.002

Linden, D. E. (2005). The P300: Where in the brain is it produced and what does it tell us? *Neuroscientist*, *11*, 563–576. doi: 10.1177/1073858405280524

Lio, G., & Boulinguez, P. (2013). Greater robustness of second order statistics than higher order statistics algorithms to distortions of the mixing matrix in blind source separation of human EEG: Implications for single-subject and group analyses. *NeuroImage*, *67*, 137–152. doi: 10.1016/j.neuroimage.2012.11.015

Lorenzo-López, L., Amenedo, E., Pascual-Marqui, R. D., & Cadaveira, F. (2008). Neural correlates of age-related visual search decline: A combined ERP and sLORETA study. *NeuroImage*, *41*, 511–524. doi: 10.1016/j.neuroimage.2008.02.041

Mitzdorf, U. (1985). Current source-density method and application in cat cerebral cortex: Investigation of evoked potentials and EEG phenomena. *Physiological Review*, *65*, 37–100.

Polich, J. (2007). Updating P300: An integrative theory of P3a and P3b. *Clinical Neurophysiology*, *118*, 2128–2148. doi: 10.1016/j.clinph.2007.04.019

Sarnthein, J., Petsche, H., Pappelsberger, P., Shaw, G. L., & Von Stein, A. (1998). Synchronization between prefrontal and posterior association cortex during human working memory. *Proceedings of the National Academy of Sciences*, *95*, 7092–7096. doi: 10.1073/pnas.95.12.7092

Schacht, A., Werheid, K., & Sommer, W. (2008). The appraisal of facial beauty is rapid but not mandatory. *Cognitive, Affective, & Behavioral Neuroscience*, *8*, 132–142. doi: 10.3758/CABN.8.2.132

Schimpf, P. H., & Liu, H. S. (2008). Localizing sources of the P300 using ICA, SSLOFO, and latency mapping. *Journal of Biomechanics, Biomedical and Biophysical Engineering*, *2*, 1–11.

Schupp, H. T., Cuthbert, B. N., Bradley, M. M., Cacioppo, J. T., Ito, T., & Lang, P. J. (2000). Affective picture processing: The late positive potential is modulated by motivational relevance. *Psychophysiology*, *37*, 257–261. doi: 10.1111/1469-8986.3720257

Sutton, S., Baren, M., Zubin, J., & John, E. R. (1965). Evoked-potential correlates of stimulus uncertainty. *Science*, *150*, 1187–1188. doi: 10.1126/science.150.3700.1187

Swick, D. (1998). Effects of prefrontal lesions on lexical processing and repetition priming: An ERP study. *Cognitive Brain Research*, *7*, 143–157. doi: 10.1016/S0926-6410(98)00019-6

Tang, A. C. (2010). Applications of second order blind identification to high-density EEG-based brain imaging: A review. In *Advances in Neural Networks—ISNN 2010* (pp. 368–377). Berlin, Germany: Springer.

Tang, A. C., Sutherland, M. T., & McKinney, C. J. (2005). Validation of SOBI components from high-density EEG. *NeuroImage*, *25*, 539–553. doi: 10.1016/j.neuroimage.2004.11.027

Werheid, K., Schacht, A., & Sommer, W. (2007). Facial attractiveness modulates early and late event-related brain potentials. *Biological Psychology*, *76*, 100–108. doi: 10.1016/j.biopsycho.2007.06.008

Wu, Y., & Zhou, X. L. (2009). The P300 and reward valence, magnitude, and expectancy in outcome evaluation. *Brain Research*, *1286*, 114–122. doi: 10.1016/j.brainres.2009.06.032

Zhang, Y., Li, X., Qian, X., & Zhou, X. L. (2012). Brain responses in evaluating feedback stimuli with a social dimension. *Frontiers in Human Neuroscience*, *6*. doi: 10.3389/fnhum.2012.00029

(Received January 29, 2013; Accepted August 23, 2013)